A NOVEL EQUATION FOR PREDICTING THE STRENGTH OF PARTICULATE POLYMER COMPOSITES

Hafizal Yazid[a,*,⋆], **Umar A. Anwar**[b], **Pairu Ibrahim**[a], **Zakaria Dris**[a], **Haniza Yazid**[c], **Sahrim Ahmad**[b] **and Muhammad Rawi Mohamed Zin**[a]

[a]*Malaysian Nuclear Agency, Bangi 43000 Kajang Selangor, Malaysia.*
[b]*Faculty of Science and Technology, Universiti Kebangsaan Malaysia, Bangi 43000 Kajang, Selangor Malaysia.*
[c]*Faculty of Electronic Engineering and Technology, Universiti Malaysia Perlis, Ulu Pauh Campus, 02600 Arau Perlis, Malaysia.*

ABSTRACT

A novel equation describes the tensile strength of particulate polymer blend composites, emphasizing crystallinity and matrix structure. It considers mechanisms of crystal nucleation, growth, and arrangement during solidification, modeling both nano- and microcomposites more effectively than previous methods. The study reveals how fillers influence crystallinity and structural morphology. Satisfying the threshold condition allows the interaction parameter χ *to be effective in the equation, enabling the relationship between spherulite size and the strength scaling factor to be established. The strong agreement between the theoretical predictions and experimental results confirms the validity and practicality of the proposed equation.*

ABSTRAK

Persamaan baru menerangkan kekuatan tegangan komposit campuran polimer zarah, menekankan kehabluran dan struktur matriks. Ia mempertimbangkan mekanisme nukleasi kristal, pertumbuhan, dan susunan semasa pemejalan, memodelkan kedua-dua nano dan mikrokomposit dengan lebih berkesan daripada kaedah sebelumnya. Kajian itu mendedahkan bagaimana pengisi mempengaruhi kehabluran dan morfologi struktur. Memuaskan keadaan ambang membolehkan parameter interaksi χ *berkesan dalam persamaan, membolehkan hubungan antara saiz sferulit dan faktor penskalaan kekuatan diwujudkan. Persetujuan kukuh antara ramalan teori dan keputusan eksperimen mengesahkan kesahihan dan kepraktisan persamaan yang dicadangkan.*

Keywords: Polymer-matrix composites (PMCs), Strength, Crystallinity, Morphology

INTRODUCTION

The strength of particulate polymer composites is critical for their engineering applications [1–3]. Traditional models, such as the rule of mixtures, often fail to predict tensile strength accurately due to complex interactions between the polymer matrix and particles. While some models consider factors like particle size distribution and interfacial bonding [4–6]. They are usually limited to microcomposites and struggle with nanocomposites. This study introduces parameters of HDPE crystallinity and structural morphology, forming a new equation to predict the strength of 60/40 NR/HDPE particulate nano and micro-filled polymer blend composites.

EXPERIMENTAL

The experiment started with sample preparation. Three main tests were conducted, and the data were analyzed to develop and validate the proposed equation.

Materials

HDPE (HI1100) with a melt flow index of 7g/10 min and a density of 0.961 g/cm^3 (Titan Chemicals Sdn. Bhd., Malaysia) and technical grade NR known as SMR L (Rubber Research Institute, Malaysia) were used. The blend's compatibilizer was produced from SMR L with a weight average molecular weight (Mw) of 4.8 x 10^5 relative to polystyrene. The filler material included nano- and microscale Boron Car- bide (Yemate Ind. Co. Limited, China) with average sizes of 20 nm and 13µm, respectively. The surfactant used was LICA 38 (Kenrich, USA) [7]. Samples prepared included a Matrix (50 wt% NR + 10 wt% LNR + 40 wt% HDPE), Nanocomposites (Matrix + nano-filler), and Microcomposites (Matrix + micro-filler), with filler content varied at 2, 4, 6, 8, and 10 wt%.

Characterizations and analysis

Based on the two main factors, HDPE crystallinity and structure morphology, the proposed equation is as follows:

$$\sigma_c = \sigma_m \chi C \tag{1}$$

$$\chi = \frac{1}{R_s} F \tag{2}$$

where σ_c is composite strength; σ_m is matrix strength; χ is interaction parameter; C is relative degree of crystallinity; R_s is ratio of crystallite size and F is spherulite size-strength scaling factor.

A set of rules was established for using the equation. Since the nucleation effect has the most significant impact on structural change and strength and it occurs at lower filler loading (as in Nanocomposite 2), the average spherulite size can be considered the nucleation size. The Matrix's average spherulite size serves as a reference. The ratio of the nucleation size to the reference, R_s, appears as $1/R_s$ in the equation. This inverse relationship indicates that a smaller size ratio correlates with higher strength. If the spherulite size meets or larger than a threshold, the strengthening effect diminishes, and the interaction parameter, χ, $f(x0) =$ is set to 1, making the equation dependent only on σm and C, typically represents microcomposites. A χ value greater than 1 signifies significant interaction, indicating that the obtained strength exceeds that of the Matrix. The spherulite size-strength scaling factor, F, is derived using data from the Matrix and Nanocomposite 2. Small Angle X-ray Scattering (SAXS) data [8] show that the filler's radius of gyration remains stable (4-5 nm) even with higher filler loadings, indicating no nano agglomeration and eliminating uncertainties from this effect.

Structural changes were identified by examining surface morphology with a Carl Zeiss GeminiSEM 500 high-resolution FESEM. This microscope, offering 1.2 nm resolution at 1 kV and 5kx magnification, was used to analyze selected samples (Matrix, Nanocomposite 2, Microcomposite 2). Matrix and Nanocomposite 2 were chosen for calibrating spherulite size and strength because their structures were easily discernible. Spherulite size was measured and analyzed using ImageJ 1.51j8 software.

XRD characterization was conducted at room temperature using a Panalytical X'pert Pro MPD diffractometer with Ni-filtered $CuK\alpha$ radiation (0.154 nm wavelength). The 2-theta range was 3^0 to 28^0 with a 0.03^0 step scan.

XRD determined the crystallinity of the HDPE phase, identified by peaks at 2 theta values of 21.43 and 23.80 for the (110) and (200) planes, respectively [9]. Natural rubber (NR) appeared as an amorphous halo. Bragg and amorphous peak profiles were fitted using deconvolution with the Pearson VII function:

$$f(x_0) = \left\{1 + \left[\frac{1}{w_0}(x_0 - c_0)^2 \left(2^{\left(\frac{1}{k_0} - 1\right)}\right)^{m_0}\right]\right\}^{-1} \qquad (3)$$

where w_0 = full width at half maximum (FWHM), c_0 = centre of the profile, x_0 = diffraction angle, k_0 = peak intensity of the profile, and m_0 = constant. The shape of this function is determined by the m_0 value; it becomes Cauchy, Lorentzian, and Gaussian when m_0 equals 1, 2, and 6 x 10^{11} respectively [10].

The crystalline fraction was determined by dividing the integrated area at the (200) reflection by the total area, which was used to estimate the degree of HDPE crystallinity at this reflection [8]. All samples underwent the same analysis procedure. The Matrix was assumed to have 100% crystallinity, with all other values expressed relative to this, termed the relative degree of crystallinity.

The uniaxial tensile data were collected using a Testometric M350 machine, operating at a crosshead speed of 50 mm/min, in accordance with ASTM D638 standards. For each composition, the average values from at least five measurements were taken, with tensile strength determined by the maximum stress observed before rupture.

RESULTS AND DISCUSSION

Surface morphology

Figures 1(a), (b), and (c) show the surface morphology results. White outlines highlight the spherulitic structures for Matrix, Nanocomposite 2, and Microcomposite 2. The spherulite areas were quantified using ImageJ 1.51j8 software, with results summarized in Tables 1. Nanocomposite 2 has the highest number of spherulites, followed by Microcomposite 2 and the Matrix, which has the fewest. Conversely, the Matrix has the largest average spherulite size, followed by Microcomposite 2, with Nanocomposite 2 having the smallest size. Notably, Nanocomposite 2 differs significantly in both spherulite size and number compared to the other samples.

It has been suggested that structural effects become significant only if the average spherulite size falls below a threshold. Based on the data, Nanocomposite 2 consistently shows spherulite sizes below 10 µm^2, establishing this as the threshold. Thus, spherulite sizes below 10 µm^2 impact strength, while sizes of 10 µm^2 and above do not. As a result, R_s and F are assigned values of 1 when there is no impact on strength.

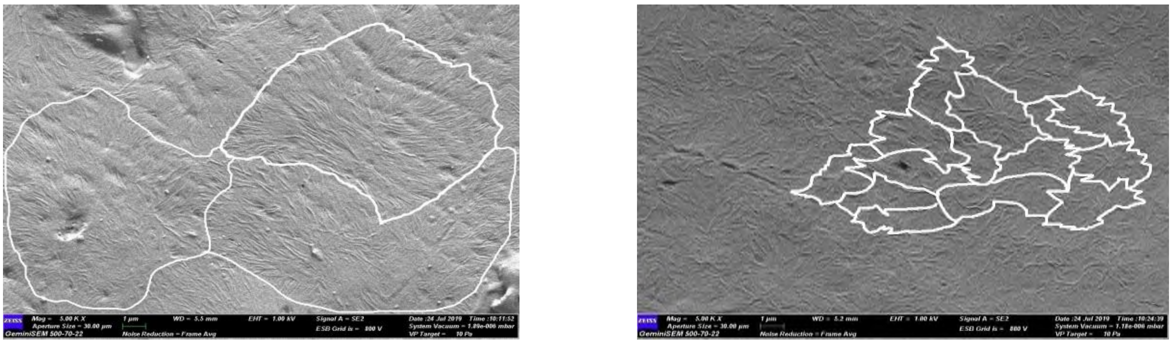

(a) Matrix (5kx).

(b) Nanocomposite 2 (5kx).

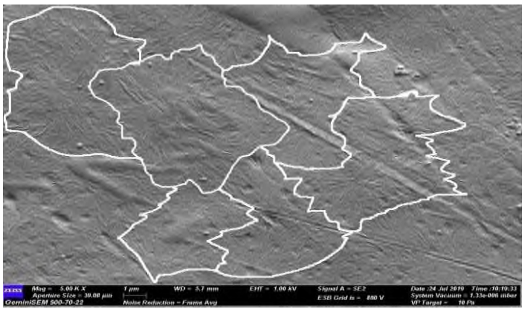

(c)Microcomposite 2 (5kx).

Figure 1: Surface morphology of samples

Table 1: Average spherulite size, R_S and F

Sample	Average size, (μm^2)	R_S	($1/R_S$)	F
Matrix	77.3 ± 3.0	1	1	1
Microcomposite 2	29.6 ± 8.1	1	1	1
Nanocomposite 2	6.3 ± 1.9	0.08	12.50	0.1409

Deconvolution output and relative degree of crystallinity (C)

Figure 2(a) illustrates the deconvolution process for the Matrix sample. The fitted data closely matched the actual measurements. Four distinct regions were successfully identified: a continuous background, an amorphous peak, crystalline peak 1, and crystalline peak 2.

The peaks comprising the samples were identified with fitting errors below 4%, indicating the success of the deconvolution process. Further calculations determined the area under the curves. Figures 2(b)–(d) provide example results using Gnuplot to plot and calculate the areas of the amorphous peak, crystalline peak 1, and crystalline peak 2. The relative degree of HDPE crystallinity at the (200) reflection was then calculated and is shown in Figure 3(a).

Figure 3(a) illustrates the trend in the relative degree of crystallinity of the samples with respect to filler loadings. Overall, the findings indicate that the addition of fillers decreases the crystallinity in all composite samples compared to the Matrix. A detailed explanation of this trend has been provided in our previous work [8]. In brief, this reduction in crystallinity is attributed to the localization and interaction of fillers, which affect the formation of crystals and the structures of HDPE in the composites.

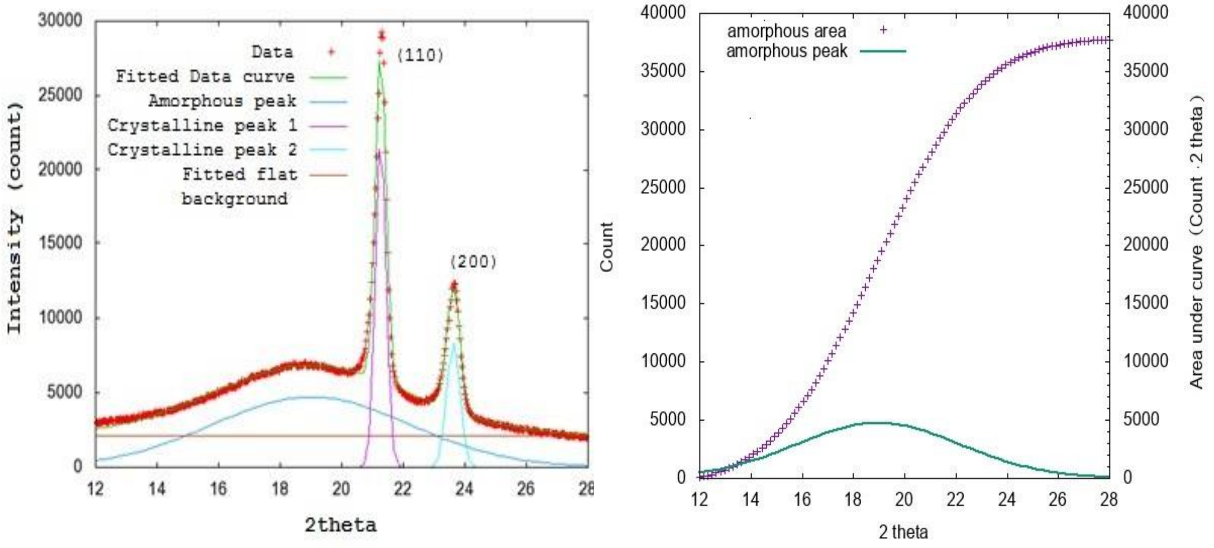

(a) Deconvolution method using Pearson VI function.

(b) Amorphous peak in Matrix sample.

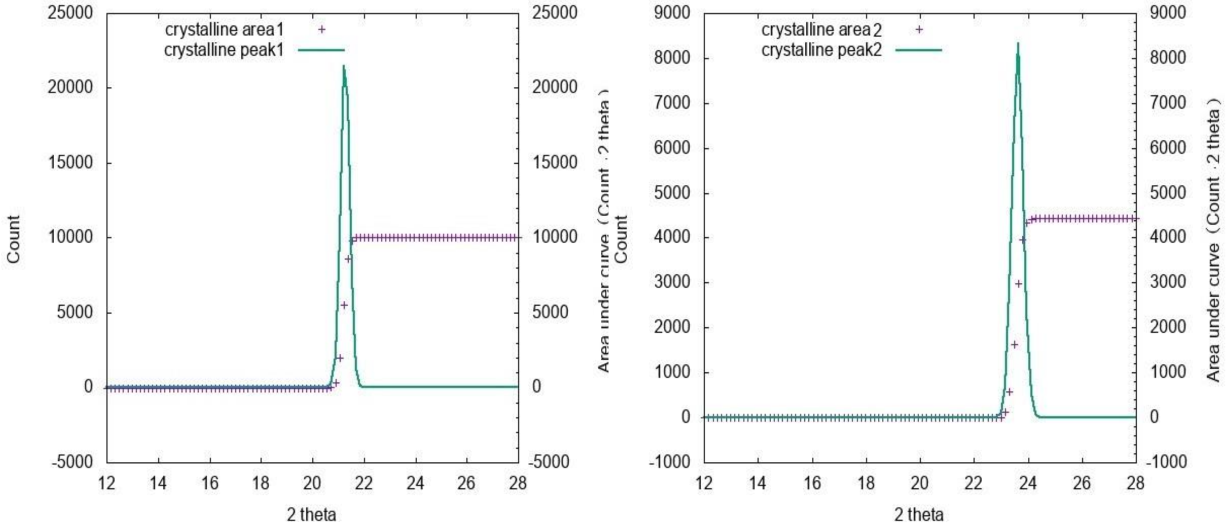

(c) Crystalline peak 1 in Matrix sample.

(d) Crystalline peak 2 in Matrix sample.

Figure 2: Result of deconvolution method and area under the curves on Matrix sample.

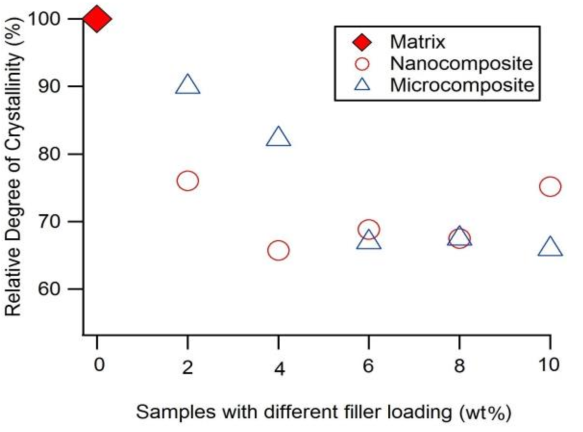

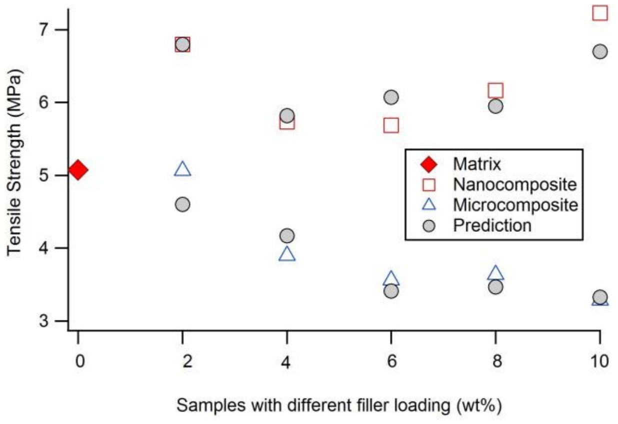

(a) Relative degree of crystallinity. experimental).

(b) Tensile strength (prediction and

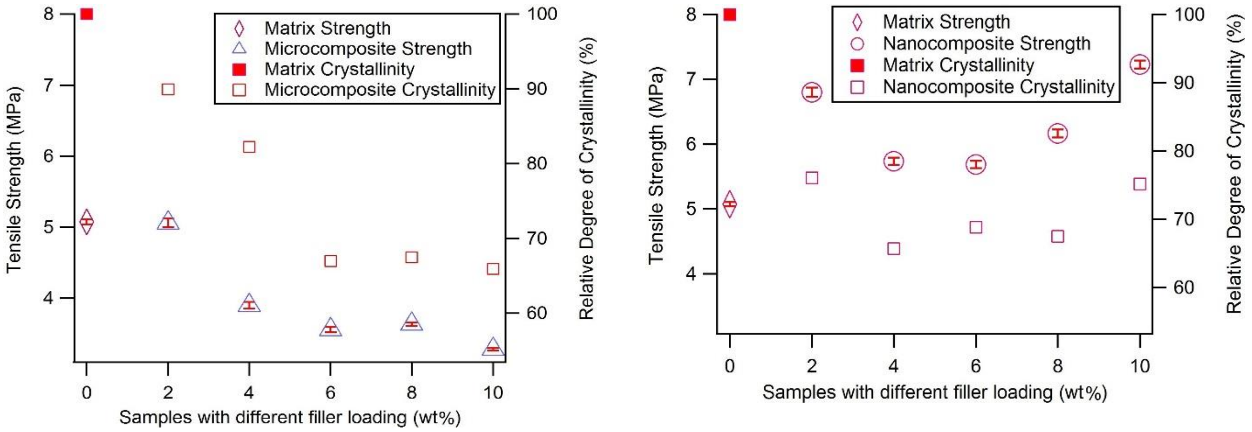

(c) Microcomposite and Matrix.

(d) Nanocomposite and Matrix.

Figure 3: Result of crystallinity, tensile strength and their comparison

Tensile strength, crystallinity and morphology

Figure 3(b) shows the tensile strength results for the Matrix, microcomposite, and nanocomposite materials. Nanocomposites exhibit superior strength compared to the Matrix and microcomposites. At 2 wt%, the tensile strength of microcomposites is nearly the same as that of the Matrix, with similar coarse structural morphology, as shown in Figures 1(a) and 1(c). Other microcomposites, with lower tensile strengths, likely have similar coarse structures. Figure 3(c) indicates two main points: the strength of microcomposites is generally lower than the Matrix, except at 2 wt%, possibly due to coarse morphology, and beyond 2 wt%, microcomposite strength aligns with crystallinity trends. Crystallinity, rather than structure, primarily affects microcomposite strength, especially above 2 wt% filler loadings. Therefore, the interaction parameter χ is set to 1 for all loadings, allowing the use of Equation (1) to predict microcomposite strength, as shown in Figure 3(b).

For nanocomposites (Figure 3(b)), the strength at 2 wt% significantly increases due to the nucleation effect. The structural morphology at this loading differs from the Matrix, exhibiting a fine structure as shown in Figures 1(a) and 1(b). Since the strengths of all nanocomposites are higher than that of the Matrix, they are expected to have a fine structure, likely with varying efficacy.

Figure 3(d) shows two key observations. First, the strength of the nanocomposites exceeds that of the Matrix and likely remains stable due to fine structural morphology until crystallinity becomes a significant factor. Second, beyond 2 wt%, the strength of nanocomposites follows the trend of crystallinity. Thus, both crystallinity and structural morphology are key factors influencing nanocomposite strength, with the effect of crystallinity becoming noticeable only above 2 wt% filler loading. The fine morphology of nanocomposites significantly affects their strength, highlighting the role of the interaction parameter χ. The term $(1/R_s)F$ or χ represents the contribution from structural changes that enhance strength, assumed to be a constant increase due to the stable radius of gyration of the filler across all loadings.

The value of F, derived from experimental data of the Matrix and Nanocomposite 2, was found to be 0.1409. Using this and the known R_s value, the interaction parameter χ was calculated to be 1.7613. This constant value applies throughout the loading range for the nanocomposite, as no nano-agglomeration occurred with increasing filler loading. Therefore, Equation (1) can be used to predict the nanocomposite's tensile strength, as shown in Figure 3(b).

Equation validation

The proposed equation is validated by comparing its calculated tensile strength values with the results from experimental data. Figure 3(b) provides a clear comparison, show- ing that the predicted tensile strength values for both micro and nanocomposites are very close to the experimental values. This demonstrates that the previous assumptions and conditions are satisfactory, enabling the proposed equation to yield reasonably accurate predictions.

CONCLUSIONS

Composite strength was influenced by both crystallinity and structural morphology. A new equation was developed to model the tensile strength of particulate polymer blend composites, effectively covering both nano- and microcomposites. This equation was validated with experimental tensile strength data, demonstrating good predictive accuracy. The approach proved effective by focusing on the matrix, which constitutes the majority of the composite's volume fraction.

ACKNOWLEDGEMENT

The authors gratefully acknowledge Malaysian Nuclear Agency and the Ministry of Higher Education (MOHE) for the financial support under the Fundamental Research Grant (FRGS/1/2018/STG07/MOSTI/02/01).

REFERENCES

[1] S. I. Hussein, A. M. Abd-Elnaiem, T. B. Asafa, H. I. Jaafar, Effect of incorporation of conductive fillers on mechanical properties and thermal conductivity of epoxy resin composite, Applied Physics A 124 (2018) 475.

[2] T. Wang, Q. Song, S. Zhang, K. Li, C. Xiao, H. Lin, Q. Shen, H. Li, Si- multaneous enhancement of mechanical and electrical/thermal prop- erties of carbon fiber/polymer composites via sic nanowires/graphene hybrid nanofillers, Composites Part A: Applied Science and Manu- facturing 145 (2021) 106404.

[3] K. B. Nilagiri Balasubramanian, T. Ramesh, Role, effect, and in- fluences of micro and nano-fillers on various properties of polymer matrix composites for microelectronics: A review, Polymers for Advanced Technologies 29 (2018) 1568–1585.

[4] J.-Z. Liang, Estimation of tensile strength of inorganic plate-like par- ticulate reinforced polymer composites, Polymer Engineering & Sci- ence 53 (2013) 1823–1827.

[5] G. Li, J. E. Helms, S.-S. Pang, K. Schulz, Analytical modeling of tensile strength of particulate-filled composites, Polymer Composites 22 (2001) 593–603.

[6] J. Liang, A. Li, Inorganic particle size and content effects on tensile strength of polymer composites, Journal of Reinforced Plastics and Composites 29 (2010) 2744–2752.

[7] O. Kwon, S. See, S. Kim, H. Hwang, Effects of surface treatment with coupling agents of pvdf-hfp fibers on the improvement of the adhesion characteristics on pdms, Applied Surface Science 321 (2014) 378–386.

[8] H. Yazid, U. A. Anwar, A. S. Zaubidah, M. Nurulizzati, M. Sabtu, M. J. Andrianny, M. Nurazila, M. R. M. Zin, R. Chen, S. Ahmad, A combined method to probe the behaviour of the filler in polymer blend nanocomposites via x-ray diffraction and thermal measurement, Nano-Structures and Nano-Objects 32 (2022) 100906.

[9] F. Yao, Q. Wu, Y. Lei, Y. Xu, Rice straw fiber-reinforced high-density polyethylene composite: Effect of fiber type and loading, Industrial Crops and Products 28 (2008) 63–72.

[10] M. Hall, Jr, V. Veeraraghavan, H. Rubin, P. Winchell, The approximation of symmetric x-ray peaks by pearson type vii distributions, Journal of Applied Crystallography - J APPL CRYST 10 (1977) 66– 68.

Declaration Of Competing Interest

The authors declare that they have no known competing personal or financial interests that could have appeared to influence the work reported in this paper.

Declaration Of Generative AI And AI-Assisted Technologies In The Writing Process

During the preparation of this work, the authors used the Grammarly service in order to perform a grammar check. After using this tool/service, the authors reviewed and edited the content as needed and take full responsibility for the con- tent of the publication.

Credit Authorship Contribution Statement

Hafizal Yazid: Conceptualization of this study, Method- ology, Data Analysis, Manuscript writing. Umar A. Anwar: Experimental work and data analysis. Pairu Ibrahim: Data analysis. Zakaria Dris: Data analysis. Haniza Yazid: Data analysis. Sahrim Ahmad: Data curation and analysis. Muhammad Rawi Mohamed Zin: Reviewing and editing.

Note:

This publication is the outcome of a research work supported by the Ministry of Higher Education (MOHE) under the grant number of FRGS/1/2018/STG07/MOSTI/02/01.

*Corresponding author

✉ hafizal@nm.gov.my (H. Yazid)

ORCID(s): 0000-0002-5559-6310 (H. Yazid) Tel:60122634647